E-ISSN 2586-9027
Homepage : https://tci-thaijo.org/index.php/SciTechAsia Science & Technology Asia
Vol.30 No.3 July - September 2025 Page: [70-77]
Original research article

Chiral Discrimination of MDPV Enantiomers by Modified β-Cyclodextrins: Molecular Docking and Semi-Empirical Study

Luckhana Lawtrakul*, Suttipong Sutsree, Jakkaphat Kaewmun

School of Bio-Chemical Engineering and Technology, Sirindhorn International Institute of Technology, Thammasat University, Pathum Thani 12120, Thailand

Received 13 May 2025; Received in revised form 22 July 2025
Accepted 30 July 2025; Available online 30 September 2025

ABSTRACT

In this study, molecular docking and PM7 semiempirical calculations were employed to investigate the binding interactions and enantiorecognition of MDPV enantiomers with various methylated β-cyclodextrins (BCDs), including heptakis(2-O-methyl)-β-cyclodextrin (2-MEB), heptakis(3-O-methyl)-β-cyclodextrin (3-MEB), heptakis(6-O-methyl)-β-cyclodextrin (6-MEB), and heptakis(2,6-di-O-methyl)-β-cyclodextrin (2,6-DIMEB). The docking simulations revealed three distinct orientations of MDPV within the cyclodextrin cavities, with the methylenedioxy and pyrrolidine rings of MDPV adopting different positions relative to the cyclodextrin rims. The calculated binding free energies (ΔG) indicated that while different orientations slightly affect binding affinity, they do not dramatically influence the stability of the host-guest complexes. Further PM7 calculations confirmed stable 1:1 inclusion complexes, with relative heats of formation ($\Delta_r H$) ranging from -41.21 to -92.29 kcal/mol. The methylation of cyclodextrins at specific hydroxyl positions played a crucial role in enhancing enantiorecognition. Notably, 6-MEB, methylated at the narrower primary hydroxyl position, exhibited the most effective enantioseparation, while 2,6-DIMEB, methylated at both rims, showed poor enantiorecognition ability. These findings emphasize the significance of selective methylation in modulating the chiral recognition capabilities of BCD derivatives.

Keywords: Binding energy analysis; Enantiorecognition; Host-guest complexes; Inclusion complex; Molecular docking

***Corresponding author:** Luckhana@siit.tu.ac.th **doi:** 10.14456/scitechasia.2025.48

1. Introduction

Enantiorecognition, the ability to distinguish between two enantiomers, is a crucial aspect of various fields, including chiral separation, drug development, and molecular sensing [1, 2]. β-Cyclodextrins (BCDs), cyclic oligosaccharides composed of seven glucose units, are widely utilized in molecular recognition processes due to their unique ability to form host-guest complexes with a variety of guest molecules [3, 4]. The selective inclusion of guest molecules within the BCD cavity can be influenced by several factors, including the geometry of the cavity and the nature of its modifications. Among the numerous derivatives of BCD, methylated BCDs have garnered significant attention for their enhanced binding properties and selective recognition capabilities [5].

In particular, the introduction of methyl groups at specific hydroxyl positions on the BCD ring has been shown to alter the size, shape, and polarity of the cavity, which can significantly impact the stereoselectivity and enantiorecognition properties of the cyclodextrin [6]. However, the relationship between the position of methylation and enantiomeric recognition remains complex and not fully understood. While previous studies have explored various BCD derivatives for enantiomer separation, limited work has been done to investigate how different methylation patterns influence the recognition of specific chiral compounds, particularly with respect to enantiomers of psychoactive substances, such as MDPV (3,4-methylenedioxypyrovalerone) [7].

This study aims to bridge this gap by employing molecular docking simulations and PM7 semiempirical calculations to investigate the binding interactions and enantiorecognition abilities of MDPV enantiomers with a series of methylated β-cyclodextrins, including heptakis(2-O-methyl)-β-cyclodextrin (2-MEB), heptakis(3-O-methyl)-β-cyclodextrin (3-MEB), heptakis(6-O-methyl)-β-cyclodextrin (6-MEB), and heptakis(2,6-di-O-methyl)-β-cyclodextrin (2,6-DIMEB). The study explores how different methylation patterns influence both the binding affinity and the enantiomeric recognition of MDPV, providing insights into the design of optimized cyclodextrin-based materials for chiral separations and selective recognition of complex enantiomers.

2. Materials and Methods

2.1 Molecular structure construction

The initial molecular structures of the cyclodextrins used as host molecules were obtained from the Cambridge Crystallographic Data Centre (CCDC) with the following identifiers: BCD, CCDC No. 1107192 [8]; 2-MEB, CCDC No. 144261 [9]; and 2,6-DIMEB, CCDC No. 118694 [10]. Modified derivatives of 3-MEB and 6-MEB were generated based on the BCD structure. The starting geometries for the enantiomers of MDPV were created by modifying the X-ray crystallographic structure of butylone (CCDC No. 1504572) [11]. Structural alterations, including the addition and removal of atoms—were performed using the Discovery Studio 2020 Client software [12].

2.1.1 Inclusion complex formation

The formation of inclusion complexes between either (R)-MDPV or (S)-MDPV enantiomers and five host molecules (BCD, 2-MEB, 3-MEB, 6-MEB, and 2,6-DIMEB) were investigated through molecular docking simulations. All docking calculations were carried out using

AutoDock software [13], employing the Lamarckian Genetic Algorithm (LGA) as the optimization protocol [14]. Input preparation for both host and guest molecules was conducted using AutoDockTools.

During the docking process, host molecules were treated as rigid structures, while guest molecules were allowed full conformational flexibility. A cubic grid box with dimensions of $15\ \mathring{A} \times 15\ \mathring{A} \times 15\ \mathring{A}$ was defined and centered on each host molecule. The grid spacing was set at $0.375\ \mathring{A}$, and default values were used for all other parameters. For each host–guest pair, 100 independent docking runs were performed. The resulting conformations were clustered based on binding pose similarities and ranked according to their predicted binding free energies (ΔG). The most energetically favorable conformation from each docking study was selected for subsequent geometry optimization.

2.1.2 Complexation energy calculation

Given the large size of the inclusion complexes (ranging from 187 to 229 atoms), the semi-empirical PM7 method was employed for geometry optimization in aqueous solution. This method provides a good balance between computational cost and accuracy for large molecular systems [15, 16].

The host, guest, and inclusion complex structures (in a 1:1 molar ratio) were fully optimized in the gas phase using PM7, as implemented in the Gaussian 16 software package [17]. The relative heats of formation ($\Delta_r H$) was calculated to evaluate the interaction strength between host and guest molecules, using the following equation:

$$\Delta_r H = \Delta H^{opt}_{cpx} - (\Delta H^{opt}_{host} + \Delta H^{opt}_{guest}). \quad (2.1)$$

Here $\Delta H^{opt}_{cpx}, \Delta H^{opt}_{host}$, and ΔH^{opt}_{guest} represent the PM7 optimized heats of formation of the inclusion complex, the isolated host molecule, and the isolated guest molecule, respectively. A more negative $\Delta_r H$ value indicates a more stable host–guest complex. These parameters were used to evaluate the suitability of the guest molecules for inclusion within the host cavity. Experimental evidence also supports the 1:1 molar ratio used in the formation of these complexes [18].

3. Results and Discussion

3.1 Molecular docking calculations

Molecular docking simulations were performed to estimate the binding free energy (ΔG) between the host molecules (cyclodextrins) and the guest molecules (MDPV enantiomers). The docking results, summarized in Table 1, indicate that the MDPV enantiomers can adopt three distinct orientations within the cavities of BCD, 6-MEB, and 2,6-DIMEB.

Table 1. The lowest free energy of binding (ΔG in kcal/mol) for each conformation in the 1:1 inclusion complex from molecular docking calculations.

	(R)-MDPV			(S)-MDPV		
	Conf. I	Conf. II	Conf. III	Conf. I	Conf. II	Conf. III
BCD	-6.17	-5.44	-5.06	-6.30	-5.88	-5.08
2-MEB	-6.85	-6.45	n/a[a]	-6.75	-6.37	n/a
3-MEB	-6.62	-5.51	n/a	-6.75	-5.59	n/a
6-MEB	-6.63	-5.80	-5.86	-6.71	-6.12	-6.03
2,6-DIMEB	-7.12	-6.20	-6.16	-7.04	-6.75	-6.27

[a] n/a is not available

In the most frequently observed orientation, Conformation I (Conf. I), both the methylenedioxy and pyrrolidine rings of MDPV are positioned near the wider, secondary hydroxyl rim of the cyclodextrins. In Conformation II (Conf. II), the methylenedioxy ring remains near the secondary rim, but the pyrrolidine ring is di-

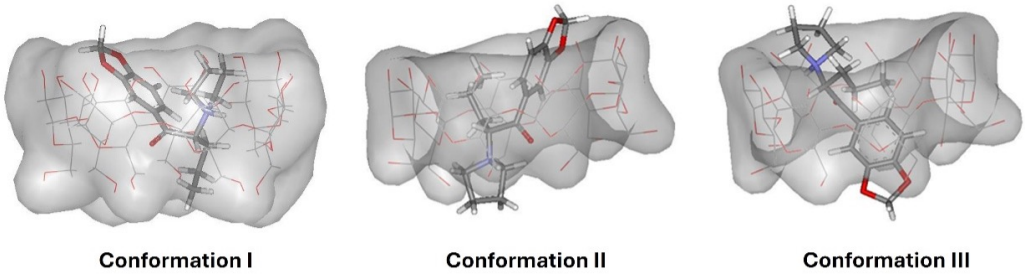

Fig. 1. Three possible orientations of the MDPV–BCD complex from molecular docking. MDPV is shown as sticks; BCD is shown as lines with a surface (probe radius: 1.4 $\mathring{A}$).

rected towards the narrower, primary hydroxyl rim. In contrast, Conformation III (Conf. III) places the MDPV molecule in the opposite orientation within the cyclodextrin cavity, as shown in Fig. 1. Notably, only Conformations I and II were observed for 2-MEB and 3-MEB.

During docking, the MDPV enantiomers were treated as flexible molecules, while the cyclodextrins were kept rigid. The calculated ΔG values for the different conformations showed only minor differences, ranging from -5.06 to -7.12 kcal/mol, with an average variation of about 2.06 kcal/mol. This suggests that while the different orientations of MDPV within the cyclodextrin cavity can slightly affect the binding affinity, they do not dramatically alter the overall stability of the host–guest complexes. The most stable complexes (those with the lowest ΔG values) for each system were selected for further optimization using the PM7 semiempirical method.

3.1.1 PM7 calculations

The PM7 calculations performed under ideal gas conditions, as summarized in Table 2, offer further insight into the energy profiles of the host–guest inclusion complexes. The relative heats of formation ($\Delta_r H$) calculated for the various systems range from –41.21 to –92.29 kcal/mol,

Table 2. The relative heats of formation ($\Delta_r H$, in kcal/mol) from PM7 calculations.

Complex	Conf.	(R)-MDPV $\Delta_r H$	Conf.	(S)-MDPV $\Delta_r H$
BCD	I	-64.41	I	-62.29
	II	-71.68	II	-67.28
	III	-69.07	III	-77.64
2-MEB	I	-72.64	I	-70.91
	II	-77.31	II	-85.60
3-MEB	I	-41.21	I	-60.46
	II	-52.06	II	-60.43
6-MEB	I	-74.74	I	-82.03
	II	-90.00	II	-78.54
	III	-92.29	III	-83.70
2,6-DIMEB	I	-55.02	I	-64.68
	II	-66.54	II	-65.70
	III	-78.03	III	-82.78

confirming that all host and guest molecules studied can form stable 1:1 inclusion complex. This work aims to investigate the effect of methylation on β-cyclodextrins (BCDs) in terms of their complexation ability and enantiorecognition of MDPV enantiomers. The role of methylation—both in terms of the degree and position of substitution—was examined by comparing the relative heats of formation differences ($|\Delta\Delta_r H|$) between the (R)-MDPV and (S)-MDPV enantiomers, as reported in Table 3.

Among the various derivatives tested, 6-MEB, which is methylated at the narrower primary hydroxyl position, showed the most effective enantioseparation of MDPV, with a $|\Delta\Delta_r H|$ of 8.59 kcal/mol and a resolution (Rs) of 1.46 at

Table 3. The lowest relative heats of formation ($\Delta_r H$) for each system, and the absolute different $\Delta_r H$ ($|\Delta\Delta_r H|$) in kcal/mol between MDPV enantiomers obtained from PM7 calculations and the resolution (Rs) based on capillary electrophoresis experiment [18].

Complex	(*R*)-MDPV		(*S*)-MDPV		$\lvert\Delta\Delta_r H\rvert$	R_s
	Conf.	$\Delta_r H$	Conf.	$\Delta_r H$		
BCD	II	-71.68	III	-77.64	5.96	No data
2-MEB	II	-77.31	II	-85.60	8.29	0.24 at 2.5 mM
3-MEB	II	-52.06	I	-60.46	8.40	0.52 at 30 mM
6-MEB	III	-92.29	III	-83.70	8.59	1.46 at 2.5 mM
2,6-DIMEB	III	-78.03	III	-82.78	4.75	0

a 2 mM concentration. This suggests that the methylation of BCD at the primary hydroxyl position significantly enhances the enantiorecognition capability, likely due to better spatial alignment with the MDPV enantiomers.

On the other hand, BCDs methylated at the wider secondary hydroxyl positions, such as 2-MEB and 3-MEB, showed only modest chiral recognition performance. Specifically, 2-MEB exhibited a $|\Delta\Delta_r H|$ of 8.29 kcal/mol and an Rs of 0.24 at 2.5 mM, while 3-MEB showed a $|\Delta\Delta_r H|$ of 8.40 kcal/mol and an Rs of 0.52 at 30 mM. These results indicate that methylation at the secondary hydroxyl positions does not provide the same level of enantiorecognition efficiency as methylation at the primary hydroxyl position, likely due to less favorable steric interactions between the host and the guest molecules.

Interestingly, 2,6-DIMEB was ineffective in discriminating against the MDPV enantiomers. The $|\Delta\Delta_r H|$ value for 2,6-DIMEB was 4.75 kcal/mol, which is lower than the $|\Delta\Delta_r H|$ of its parent BCD (5.96 kcal/mol). This suggests that the methylation of both the primary and secondary hydroxyl groups in 2,6-DIMEB may lead to reduced binding affinity and poorer chiral recognition ability compared to the non-methylated BCD or selectively methylated derivatives. These findings highlight the critical role of the position and degree of methylation in determining the enantiorecognition performance of BCD derivatives, emphasizing that selective modification of the primary hydroxyl groups can enhance the chiral discrimination of MDPV enantiomers.

3.2 Molecular interpretations

Upon full optimization, the most frequently observed conformation, Conf. I, where both the methylenedioxy and pyrrolidine rings of MDPV are positioned near the wider rim of the cyclodextrin, does not correspond to the lowest relative heats of formation ($\Delta_r H$) for each system (Table 2). In contrast, Conf. II is favored when the methylated substituent is located at the wider rim (e.g., 2-MEB and 3-MEB), while Conf. III is preferred when the methylated substituent is at the narrower rim (e.g., 6-MEB). This preference is attributed to the position of MDPV's methylenedioxy ring, which aligns with the methyl groups on the respective rims. Specifically, the longer tail of 6-CH2OMe compared to 2-OMe provides greater flexibility, allowing for a more favorable interaction with MDPV's methylenedioxy ring. As a result, Conf. III is the most favorable conformation for the 2,6-DIMEB complex, exhibiting the lowest complexation energy (Table 3).

The inclusion complexes of MDPV enantiomers with 2-MEB, 6-MEB, and 2,6-DIMEB were selected for further investigation due to their effective separation capabilities and not identical migration order

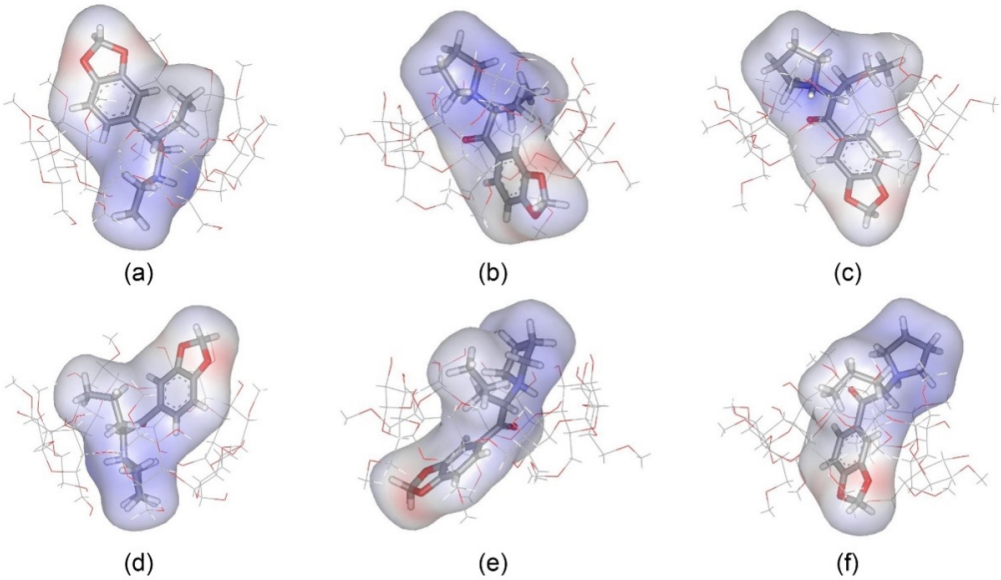

Fig. 2. The optimized PM7 models of the 1:1 inclusion complex. Host molecules are shown in line models while MDPV enantiomers are shown as stick models with a 1.4 Å probe radius: (a) 2-MEB/(R)-MDPV Conf. II; (b) 6-MEB/(R)-MDPV Conf. III; (c) 2,6-DIMEB/(R)-MDPV Conf. III; (d) 2-MEB/(S)-MDPV Conf. II; (e) 6-MEB/(S)-MDPV Conf. III; (f) 2,6-DIMEB/(S)-MDPV Conf. III.

in chromatographic analyses. These complexes are stabilized by a combination of electrostatic dipole-dipole interactions, van der Waals forces, and hydrophobic interactions (see Fig. 2). Importantly, no hydrogen bonding between MDPV and the host molecules was observed.

In the case of 2-MEB, the (S)-MDPV enantiomer forms a more stable complex within the cyclodextrin cavity compared to (R)-MDPV, exhibiting a lower binding affinity of 8.29 kcal/mol (Table 3), despite their similar binding modes (Figs. 2a, d). This suggests that (S)-MDPV is more effectively accommodated within the 2-MEB cavity than (R)-MDPV. On the other hand, in the 6-MEB/MDPV complexes, the methylenedioxy ring of MDPV is positioned inside the cavity near the narrower rim, with the hydrophobic tails of the 6-CH_2OMe groups extending into the cavity from the glucose units (1, 2, and 4), see Figs. 2b, and 2e. This arrangement leads to a more stable inclusion complex, with relative heats of formation ranging from -83.70 to -92.29 kcal/mol (Table 3). This difference in stability results in distinct enantioseparation behaviors: in the 2-MEB system, (R)-MDPV migrates first due to its weaker binding affinity, whereas in the 6-MEB system, (S)-MDPV migrates first because of its lower binding affinity compared to (R)-MDPV.

Although the 2,6-DIMEB complex favors Conf. III, similar to 6-MEB, it does not exhibit significant enantioseparation ability for MDPV enantiomers, as indicated by the relatively small difference in $\Delta\Delta_r H$ (only 4.75 kcal/mol). This suggests that 2,6-DIMEB forms inclusion complexes

with both (R)-MDPV and (S)-MDPV with comparable binding affinities. This reduced enantioseparation efficiency may be due to the methylated groups on both rims of the cyclodextrin, which increase its flexibility and allow it to accommodate both enantiomers of MDPV similarly.

4. Conclusion

This study highlights the critical role of methylation in modulating the enantiorecognition capabilities of β-cyclodextrin derivatives for MDPV enantiomers. The molecular docking and PM7 calculations revealed that MDPV enantiomers can adopt different orientations within the cyclodextrin cavities, with the most stable complexes favoring the conformations where the methylenedioxy ring of MDPV aligns with the methylated hydroxyl groups. Selective methylation at the primary hydroxyl group (as in 6-MEB) significantly enhances the enantiorecognition of MDPV, while methylation at both rims (as in 2,6-DIMEB) results in a reduced enantiorecognition ability, likely due to increased flexibility of the cyclodextrin cavity. These results provide valuable insights into the design of cyclodextrin-based materials for chiral separation and recognition, suggesting that careful control of methylation position can optimize the performance of cyclodextrins in enantiomeric discrimination.

Acknowledgements

This study was supported by Thammasat University Research Fund, contract No. TUFT 75/2568.

References

[1] Gogoi A, Mazumder N, Konwer S, Ranawat H, Chen NT, Zhuo GY. Enantiomeric recognition and separation by chiral nanoparticles. Molecules. 2019;24(6):1007.

[2] de Koster N, Clark CP, Kohler I. Past, present, and future developments in enantioselective analysis using capillary electromigration techniques. Electrophoresis. 2021;42(1-2):38–57.

[3] Cid-Samamed A, Rakmai J, Mejuto JC, Simal-Gandara J, Astray G. Cyclodextrins inclusion complex: preparation methods, analytical techniques and food industry applications. Food Chem. 2022;384:132467.

[4] Szente L, Szemán J. Cyclodextrins in analytical chemistry: host–guest type molecular recognition. Anal Chem. 2013;85(16):8024–30.

[5] Lawtrakul L, Toochinda P. Chiral recognition of butylone by methylated β-cyclodextrin inclusion complexes: molecular calculations and two-level factorial designs. ACS Omega. 2025;10:2003–11.

[6] Fenyvesi É, Szemán J, Csabai K, Malanga M, Szente L. Methyl-beta-cyclodextrins: the role of number and types of substituents in solubilizing power. J Pharm Sci. 2014;103(5):1443–52.

[7] Baumann MH, Bukhari MO, Lehner KR, Anizan S, Rice KC, Concheiro M, et al. Neuropharmacology of 3,4-methylenedioxypyrovalerone (MDPV), its metabolites, and related analogs. Curr Top Behav Neurosci. 2017;32:93–117.

[8] Steiner T, Koellner G. Crystalline β-cyclodextrin hydrate at various humidities: fast, continuous, and reversible dehydration studied by X-ray diffraction. J Am Chem Soc. 1994;116(12):5122–8.

[9] Pitha J, Harata K. CCDC 144261: Experimental crystal structure determination [Internet]. Cambridge: Cambridge Crystallographic Data Centre; 2004

[cited 2025 Aug 23]. Available from: https://doi.org/10.5517/cc4v3ln

[10] Aree T, Hoier H, Schulz B, Reck G, Saenger W. Novel type of thermostable channel clathrate hydrate formed by heptakis(2,6-di-O-methyl)-β-cyclodextrin·15H_2O – a paradigm of the hydrophobic effect. Angew Chem Int Ed Engl. 2000;39(5):897–9.

[11] Wood MR, Bernal I, Lalancette RA. The hydrochloride hydrates of pentylone and dibutylone and the hydrochloride salt of ephylone: the structures of three novel designer cathinones. Struct Chem. 2017;28(5):1369–76.

[12] BIOVIA Discovery Studio Visualizer [Internet]. San Diego: Dassault Systèmes; 2020 [cited 2025 Aug 23]. Available from:https://discover.3ds.com/discovery-studio-visualizer-download.

[13] Morris GM, Huey R, Lindstrom W, Sanner MF, Belew RK, Goodsell DS, et al. AutoDock4 and AutoDockTools4: Automated docking with selective receptor flexibility. J Comput Chem. 2009;30(16):2785–91.

[14] Fuhrmann J, Rurainski A, Lenhof HP, Neumann D. A new Lamarckian genetic algorithm for flexible ligand–receptor docking. J Comput Chem. 2010;31(9):1911–8.

[15] Christensen AS, Kubař T, Cui Q, Elstner M. Semiempirical quantum mechanical methods for noncovalent interactions for chemical and biochemical applications. Chem Rev. 2016;116(9):5301–37.

[16] Triamchaisri N, Toochinda P, Lawtrakul L. Structural investigation of beta-cyclodextrin complexes with cannabidiol and delta-9-tetrahydrocannabinol in 1:1 and 2:1 host–guest stoichiometry: molecular docking and density functional calculations. Int J Mol Sci. 2023;24(3):1525.

[17] Frisch MJ, Trucks GW, Schlegel HB, Scuseria GE, Robb MA, Cheeseman JR, et al. Gaussian 16, Revision C.01. Wallingford (CT): Gaussian Inc.; 2016.

[18] Varga E, Benkovics G, Darcsi A, Várnai B, Sohajda T, Malanga M, et al. Comparative analysis of the full set of methylated β-cyclodextrins as chiral selectors in capillary electrophoresis. Electrophoresis. 2019;40(21):2789–98.